International Journal of Applied Mathematics and Engineering Sciences
Vol. 3, No.2 (July-December, 2018)

APPLICATION OF THE EMPIRICAL MODE DECOMPOSITION FOR SYSTEM IDENTIFICATION AND STRUCTURAL HEALTH MONITORING

N. Cheraghi & F. Taheri

Received: 13rd August 2017 Revised: 24th December 2017 Accepted: 10th March 2018

ABSTRACT: When measured vibration data of a structural response contains damage related data, it is crucial to extract as much damage related information as possible. This paper presents an analytical and numerical investigation into the applicability of the empirical mode decomposition (EMD) for structural damage detection caused by a sudden change of structural stiffness, in conjunction with a novel idea based on energy of *intrinsic mode functions (IMFs).* A 6-DOF mechanical system was modeled and analyzed subject to an impact load by exact solution, using MATLAB software, as well as with the finite element method, using the ANSYS program. The system's natural frequency and damping ratio were evaluated. A proposed damage index was utilized to detect the presence of damage.

Keywords: Damping, plastics, empirical mode decomposition, computation, materials.

INTRODUCTION

Vibration-based structural damage detection methods have attracted considerable attention in recent years for health monitoring of large civil structures (Xu *et al.*, 2004). Most of the currently used vibration-based structural damage detection methods are formulated based on the idea that the measured modal parameters, or the properties derived from these modal parameters, are functions of the physical properties of the structure. As a result, changes in the physical properties will cause noticeable and detectable changes in the modal parameters (Deobling *et al.* (1996). Although these methods have demonstrated a certain degree of success in damage detection of small structures, there are several confounding factors that make the applicability and effectiveness of these methods for health monitoring of larger structures is rather questionable. One issue of primary concern is that these methods presume access to a set of data extracted from the structure at its undamaged (healthy) state; however, such information is not usually readily available in the case of most existing civil structures. Another factor is that most of these methods operate based on the data recorded before and after the occurrence of the damage. Moreover, often a linear structural behaviour is assumed for the structure during the data collection. On the contrary, the identified modal parameters (the damage indices) in fact represent the average characteristics of the structure over the duration of the data collection, thus they may not be acutely sensitive to damage, since damage is typically a local phenomenon. Consequently, if a damage event suddenly occurs during the measurement period, the time of the occurrence of the damage cannot be determined by these methods.

In contrast to a large number of publications pertaining to damage indices using the average modal characteristics, there is a paucity of research works addressing instantaneous damage indices. It is believed that the application of time–frequency data processing would be necessary to detect a damage event, including characterization of the event time. The logical candidates for such a task would be the wavelet method, and the recently emerged signal processing technique, as well as the empirical mode decomposition (EMD), introduced by Huang *et al.* (1998, 1999).

There have been several studies devoted to detection of damage by various signal processing method. For a comprehensive analysis of such publication the reader should consult Cheraghi (2006). Nevertheless, those studies, using either the wavelet analysis or the EMD approach are based on numerical simulations. Several of the important assumptions made through such analyses will require further investigation and verification. It is

therefore desirable to verify the integrity of these approaches by laboratory-scale experimental investigations before their application in large structures could be fully justified.

BACKGROUND TO THE HILBERT-HUANG TRANSFORM (HHT)

One of the most widely used dynamic data processing tools is the Fourier Transform (FT) and its digital analogue, the Fast Fourier Transform (FFT). The FT (developed decades ago) and its fairly recently developed counterpart, the FFT carry strong *a-priori* assumptions about the source of data, such as linearity and stationary properties. Natural phenomena responses are essentially nonlinear and non-stationary. The accommodation of this fact in FFT-based analysis often involves using more data samples to assure acceptable convergence and non-algorithmic procedural steps in the interpretation of FFT results. Therefore they cannot be considered as the most optimum methods for studying non-linear waves and other nonlinear phenomena.

Wavelet-based analysis yields some improvement over the FFT, because it can handle non-stationary data, but the limitation of a linear data set remains constant. Wavelet methods may also prove inadequate because although being wellsuited for analyzing data with gradual frequency changes, its non-locally adaptive nature causes leakage. This leakage can spread frequency energy over a wider range, removing the details of data and thus giving it an overly smooth appearance.

To overcome these shortfalls, the Empirical Mode Decomposition method was recently proposed (Huang *et al.* (1998, 1999)). This method is based on the use of the Hilbert-Huang Transform (HHT), and provides a novel approach to the solution of the nonlinear class of problems. The initial application of the method was used to analyze hydrospheric processes. The HHT allowed direct algorithmic analysis of nonlinear and non-stationary data functions by using an engineering and *a posteriori* data processing method, namely an Empirical Mode Decomposition method (EMD). A key feature of the signal analysis based on HHT is its physical attributes, which has made the method popular to a wide range of researchers and experts in signal processing and other related fields.

Several works based on the framework of HHT theory have been reported in the recent years (Deng *et al.*, (2001), and Flandrin *et al.*, (2004)). Its application for signal analysis have spread into earthquake research (Loh *et al.* (2001), ocean science (Huang, (1999), biomedicine (Huang *et al.*, (1998, 1999), Phillips (2003)), speech signal analysis, and image analysis and processing (Han *et al.* (2003).

MATHEMATICAL DESCRIPTION OF THE HHT

The HHT method consists of two parts: (1) the *Empirical Mode Decomposition (EMD)*, and (2) the *Hilbert Spectral Analysis.* As stated earlier, with EMD, one can decompose any complicated data set into a finite and often less complicated *intrinsic mode functions (IMFs).* An IMF is defined as a function satisfying the following conditions:

(a) The number of extrema and the number of zero-crossings must either equal or differ at most by one in the signal function being considered;

(b) At any point, the mean value of the envelope defined by the local maxima and the envelope defined by the local minima should be zero.

The resulting IMF then would admit a well-behaved Hilbert transform. In this way therefore EMD decomposes signals adaptively and is applicable to nonlinear and non-stationary data (the fundamental theory on nonlinear time series can be found in Huang *et al.*, (1998). In this section, only a brief introduction is given to make this paper somewhat self-contained. The readers are referred to Huang *et al.* (1998) for details.

The Hilbert transform, $Y(t)$, of an arbitrary function, $X(t)$, in Lp-class (Titchmarsh 1948), is defined by:

$$Y(t) = \frac{1}{\pi} P \int_{-\infty}^{\infty} \frac{X(t')}{t - t'} dt' \qquad (1)$$

where P indicates the Cauchy principal value. Consequently an analytic signal, $Z(t)$, can be produced by:

$$Z(t) = X(t) + iY(t) = a(t)e^{i\theta(t)} \tag{2}$$

where

$$a(t) = [X^2(t) + Y^2(t)]^{\frac{1}{2}} \text{ and } \theta(t) = \arctan\left(\frac{Y(t)}{X(t)}\right) \tag{3}$$

are the instantaneous amplitude and phase angle of $X(t)$.

Since Hilbert transform $Y(t)$ is defined as the convolution of $X(t)$ and $t/1$ by Equation(1), it emphasizes the local properties of $X(t)$, even though the transform is global. In Equation (2), the polar coordinate expression further clarifies the local nature of this representation. With Equation (2), the instantaneous frequency of $X(t)$ can be defined by:

$$\omega(t) = \frac{d\theta(t)}{dt} \tag{4}$$

However, there is still considerable controversy on this definition. A detailed discussion and justification of the above definition can be found in Huang et al., (1998).

EMD is a necessary pre-processing of the data before the Hilbert transform can be applied. It reduces the data into a collection of *IMF*s and each *IMF*, which represents a simple oscillatory mode, is a counterpart to a simple harmonic function, yet is more general.

Moreover, by the application of EMD, any signal $X(t)$ can be decomposed into a series of finite IMFs, or $\text{imf}_j(t)$ ($j = 1; \ldots ; n$), and a residue, $r(t)$, where n is a nonnegative integer depending on $X(t)$; that is,

$$X(t) = \sum_{j=1}^{n} imf_j(t) + r(t) \tag{5}$$

Let $Xj(t) = \text{imf}_j(t)$, whose corresponding instantaneous amplitude, $a_j(t)$, and frequency, $\omega_j(t)$, can be computed by Equations (3) and (4). Through Equations (2) and (4), the $\text{imf}_j(t)$ can be expressed as the real part (RP), in the following form:

$$imf_j(t) = RP\left[a_j(t)\exp(i\int \omega_j(t)dt)\right] \tag{6}$$

Therefore, using Equations (5) and (6), $X(t)$ can be expressed as the IMF expansion as follows:

$$X(t) = RP\left[\sum_{j=1}^{n} a_j(t)\exp(i\int \omega_j(t)dt) + r(t)\right] \tag{7}$$

which generalizes the following Fourier expansion by admitting variable amplitudes and frequencies

$$X(t) = \sum_{j=1}^{n} a_j e^{i\omega_j t} \tag{8}$$

Consequently, the main advantage of EMD over FFT is that it could effectively accommodate nonlinear and non-stationary data. Equation (7) thus enables one to represent the amplitude and the instantaneous frequency as a function of time in a threedimensional plot, in which the amplitude is contoured on the time-frequency plane.

MODAL RESPONSE OF *n*-DOF STRUCTURES DUE TO IMPULSE LOADING

The equation of motion of an n-DOF structure can be expressed as

$$M\ddot{X}(t) + C\ddot{X}(t) + KX(t) = F(t) \tag{9}$$

in which $X(t) = [x_1, x_2, \ldots, x_n]$ is the displacement vector, $F(t)$ is the excitation vector and M, C, and K are the mass, damping, and stiffness matrices, respectively. With the assumption of the existence of normal modes, the displacement and acceleration responses can be decomposed into n real modes

$$\sum_{j=1}^{n} \phi_j Y_j(t); \qquad \ddot{X}(t) = \sum_{j=1}^{n} \phi_j \ddot{Y}(t) \tag{10}$$

In the above equation, it is apparent that the $n \times n$ mode-shape matrix ϕ serves to transform the generalized coordinate vector Y to the geometric coordinate vector X. The generalized components in vector Y are called the normal coordinates of the structures.

Substituting Equation (10) into Equation (9) and using the orthogonal properties of the mode shapes, one can decouple Equation (9) into n modes

$$\ddot{Y}_j + 2\xi_j \omega_j \dot{Y} + \omega_j^2 Y = \phi_j^T F(t)/m_j \tag{11}$$

in which ω_j is the j^{th} modal frequency, ξ_j is the j^{th} modal damping ratio, and m_j is the j^{th} modal mass. Consider an impact loading applied to the p^{th} DOF of the system, i.e. $f_p(t) = F_0\,\delta(t)$ and $f_j(t) = 0$ for all $j \neq p$, where $f_j(t)$ is the jth element of $F(t)$.

Further manipulation of the above equation (details are provided in Cheraghi (2006)), will yield the following equations:

$$A_{kj}(t) \frac{F_0 \left|\phi_{kj}\right| \left|\phi_{pj}\right| \omega_j}{m_j \sqrt{1-\xi_j^2}} \frac{e^{-\xi_j \omega_j t} \left(\sqrt{(\xi_j^2 \omega_j^2 + \omega_{dj}^2)^2 + 4\xi_j^2 \omega_j^2 \omega_{dj}^2} \right)}{\left(\xi_j^2 \omega_j^2 + \omega_{dj}^2 \right)^2} \tag{12}$$

$$\beta_{kj}(t) = \omega_{dj} t + \varphi_j + \frac{\pi}{2} + \varphi_{kj,p} - \theta \tag{13}$$

In the above Equations $\varphi_{kj,p}$ is the phase difference between the k^{th} element and the p^{th} element in the j^{th} mode shape. With the existence of normal modes, all the mode shapes are real and hence $\varphi_{kj,p}$ is either $\pm 2m\pi$ or $\pm (2m+1)\pi$ where m is an integer, i.e.

$$\varphi_{kj}/\varphi_{pj} \succ 0 \text{ when } \varphi_{kj,p} = \pm\, 2m\pi$$
$$\varphi_{kj}/\varphi_{pj} \prec 0 \text{ when } \varphi_{kj,p} = \pm\, (2m+1)\pi$$

From Equations (12) and (13), one can obtain

$$\ln A_{kj}(t) = -\xi_j \omega_j t + \ln \left(\frac{F_0 \left|\phi_{kj}\right| \left|\phi_{pj}\right| \omega_j}{m_j \sqrt{1-\xi_j^2}} \frac{\left(\sqrt{(\xi_j^2 \omega_j^2 + \omega_{dj}^2)^2 + 4\xi_j^2 \omega_j^2 \omega_{dj}^2} \right)}{\left(\xi_j^2 \omega_j^2 + \omega_{dj}^2 \right)^2} \right) \tag{14}$$

$$\omega_j(t) = d\beta_{kj}(t)/dt = \omega_{dj} \tag{15}$$

As seen with the measured impulse response vector, the EMD method can be used to decompose each measurement into n modal responses. Then, each modal response can be processed through the Hilbert transform to determine the instantaneous amplitude and phase angle. Finally, the system identification can be completed, including natural frequencies, damping ratios, mode shapes, mass matrix, damping matrix, and stiffness matrix. In the following section, the application of the abovementioned procedure will be seen through a case study.

Case Study # 1: a Healthy (Undamaged) Structure

To investigate the effectiveness and integrity of the application of the proposed system identification for damage detection methodology in a structural system, the integrity of the Hilbert-Huang approach is investigated by applying it onto a 6-DOF mechanical?. Later, the same system will be investigated bearing a damage.

Consider the 6-DOF mechanical system, as shown in Figure 1, with the following properties:

$$m_1 = m_2 = m_3 = m_4 = m_5 = m_6 = 1\ kg$$
$$k_1 = k_2 = k_3 = k_4 = k_5 = k_6 = k_7 = 7500\ N/m,$$
$$c_1 = c_2 = c_3 = c_4 = c_5 = c_6 = c_7 = 0.75\ Ns/m$$

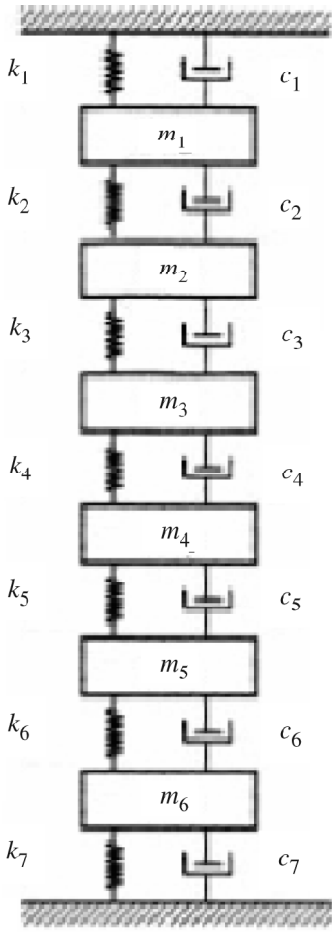

Figure 1: Schematic of the 6-DOF Mechanical System

The Hilbert-Huang spectral approach, with its procedure outlined as above, will be applied to the system. In this problem, the displacement impulse responses of all masses in response to an impact load applied to the third mass are measured. ANSYS finite element software was used to model the system, and modal and transient dynamic analyses were conducted. The results of the finite element analyses were compared to those reached through the exact solution, which were obtained using MATLAB software. The measured displacement $X_3(t)$, is shown in Figure (2a). The Fourier transforms of the displacement responses of all degrees of freedom of the system ($X_1(t)$ through $X_6(t)$) is shown in Figure (2b). The modal frequency ranges are summarized in below:

(1) $5.38\ Hz = \omega_{1L} \prec \omega_1 \prec \omega_{1H} = 6.88$ for the first mode

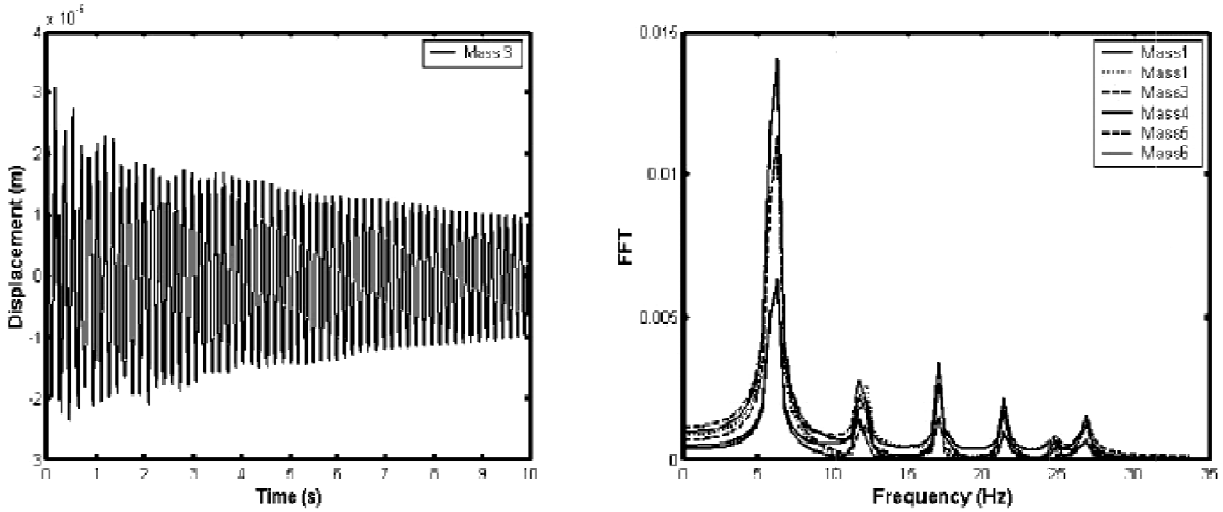

Figure 2: Plots of (a) the Displacement Impulse Response of Mass # 3 of the Damaged Mechanical System, (b) The Fourier Transform of Displacement Response of all Masses of the Healthy Mechanical System

(2) $11.21 = \omega_{2L} \prec \omega_2 \prec \omega_{2H} = 12.21$ for the second mode

(3) $16.44 = \omega_{3L} \prec \omega_3 \prec \omega_{3H} = 17.94$ for the third mode

(4) $20.8 = \omega_{4L} \prec \omega_4 \prec \omega_{4H} = 22.3$ for the fourth mode

(5) $24.08 = \omega_{5L} \prec \omega_5 \prec \omega_{5H} = 25.58$ for the fifth mode

(6) $26.12 = \omega_{6L} \prec \omega_6 \prec \omega_{6H} = 27.62$ for the sixth mode

Subsequently, the band-pass method was used to carry out the EMD calculations and to extract the IMFs. The procedure is as follows:

- The signal for each DOF ($X(t)$, shown in Figure 2a was passed through a fourthorder band-pass filter, each within the frequency band noted in above. The resulting six time histories from each DPF are denoted by X_{mj} (j = 1, 2, 3, 4, 5, 6) for each corresponding mass number.
- Then, all of the resulting X_{mj} were processed through EMD and the first IMF was used to identify the modal response of X_{mj}. As an illustration, the signature of the 4th DOF (mass) and its IMF is illustrated in Figure 3. It is important to note that the band-pass filter used for the operation should have the smallest possible phase shift to produce the best results. It should be noted that due to the phase shift, a segment of the modal response near t = 0 is not a decaying function. Such a segment should be discarded prior to the application of the Hilber transform.
- After removing this segment, the modal responses illustrated in Figure 4 are processed through the Hilbert transform and the instantaneous phase angles $\theta_{mj}(t)$ and $a_{mj}(t)$ are obtained. The plots of θ_{11} and θ_{16} versus time t for the first mass are illustrated as the dotted curves in Figures 4a and b, respectively.
- Slopes of these curves represent the first and sixth natural frequencies of the system. Figures 5a and b illustrate the plots of logarithm of the amplitude of the first and sixth DOF ($\ln a_{11}$ and $\ln a_{16}$) versus time. The linear least-square fits of the curves are also shown in the above noted figures by the solid lines. The natural frequencies ω_1 and ω_6, and the damping ratios ξ_1 and ξ_6 can be extracted from the slopes of the least square lines, as outlined earlier.
- The above process was repeated for all six DOF, and the natural frequencies and damping ratios of all DOF were obtained. The results are outlined in Table 1.

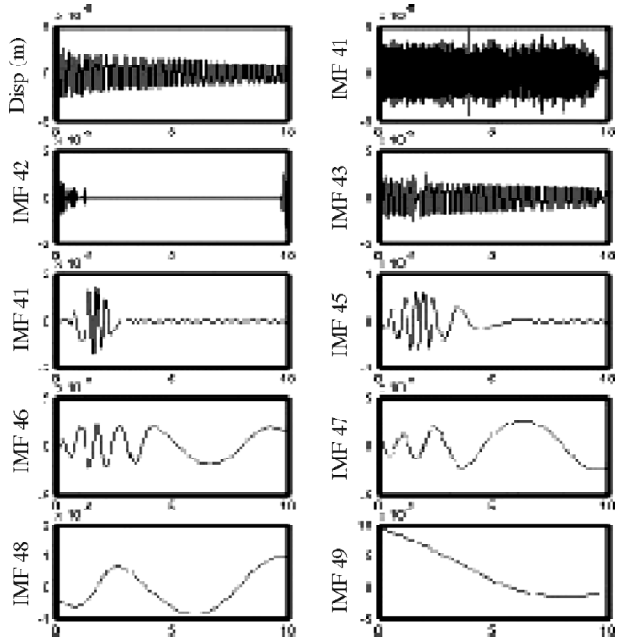

Figure 3: Displacement and IMFs of Mass #4 of the Healthy Mechanical System

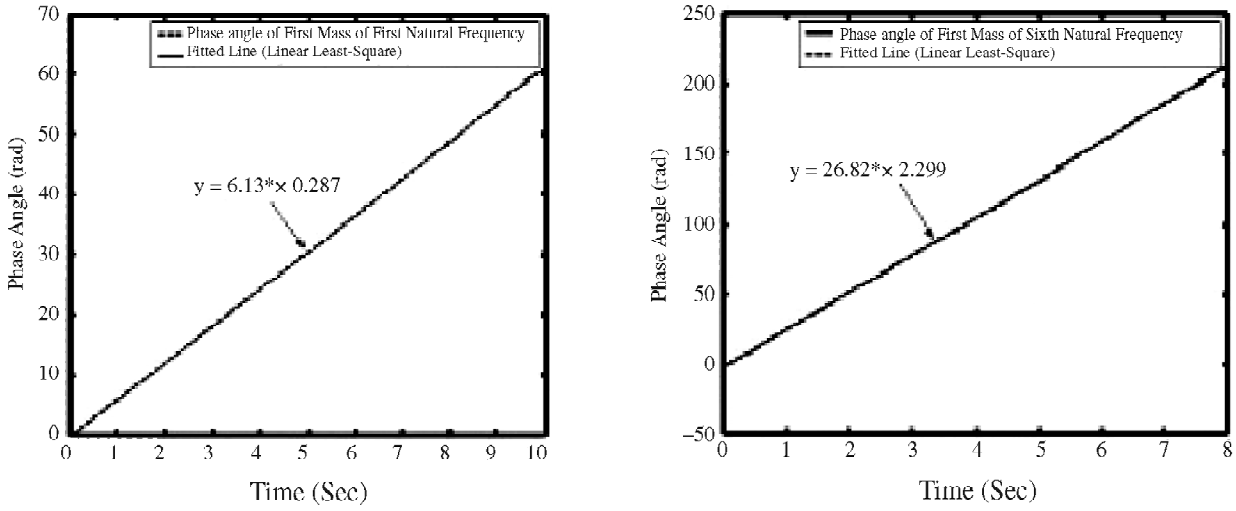

Figure 4: Plots of (a) the Unwrapped Phase Angle of the First Mass for the First Modal Response, (b) The Unwrapped Phase Angle of the First Mass for the Sixth Modal Response of the Healthy System

Table 1
Natural frequency and damping ratios of the healthy six DOF mechanical systems

Mode	*Theoretical Values*		*Identified Values*	
	Frequency (Hz)	*Damping ratio*	*Frequency (Hz)*	*Damping ratio*
1	6.13	0.19	6.13	0.19
2	11.96	0.38	11.95	0.38
3	17.18	0.54	17.17	0.54
4	21.55	0.68	21.50	0.68
5	24.84	0.78	24.81	0.79
6	26.87	0.84	26.70	0.85

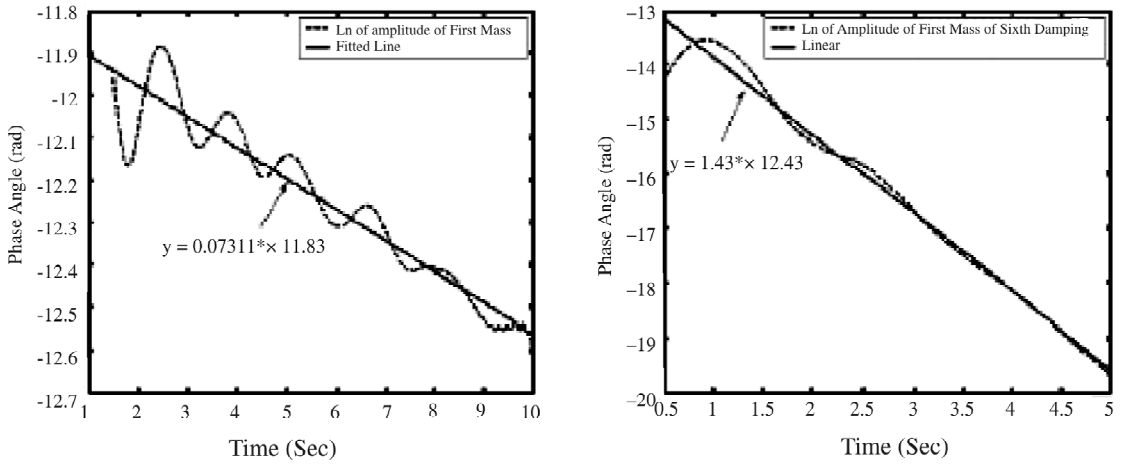

Figure 5: Plots of (a) ln Amplitude of the First Mass for the First Mode, (b) ln Amplitude of the First Mass for the Sixth Mode

It is observed from this table that the correlation between the theoretical values (frequencies and damping) and the identified results is excellent. The efficiency of the procedure can be better appreciated by noting that only one response (displacement or acceleration), measured through only one sensor, was used to generate all the natural frequencies and damping ratios of the system. It should also be noted that the results presented in Table 1 are based on averaging the mass of the system per segment.

Moreover, the complete mass matrix of the system can be calculated by repeating the above procedures for each DOF of the system. For illustration, the calculated mode shapes and their comparison with those obtained through the closed-form solution are tabulated in Table 2. The second and third modal responses are illustrated graphically in Figures 6a and b. The identified stiffness matrix and damping matrices, as well as those obtained theoretically, are listed below:

Table 2
Theoretical and Identified Mode Shapes of the Healthy six DOF Mechanical Systems

Theoretical values of the mode shapes							*Identified values of the mode shapes*					
DOF	*First*	*Second*	*Third*	*Fourth*	*Fifth*	*Sixth*	*First*	*Second*	*Third*	*Fourth*	*Fifth*	*Sixth*
1	1	1	1	1	1	1	1	1	1	1	1	1
2	1.80	1.25	0.44	–0.44	–1.25	–1.80	1.72	1.25	0.44	–0.44	–1.20	–1.80
3	2.25	0.55	–0.80	–0.80	0.55	2.25	2.27	0.55	–0.80	–0.80	0.51	2.26
4	2.25	–0.55	–0.80	0.80	0.55	–2.25	2.27	–0.55	–0.80	0.80	–0.51	2.26
5	1.80	–1.25	0.44	0.44	–1.25	1.80	1.72	–1.25	0.44	0.44	1.20	1.80
6	1	–1	1	–1	1	–1	0.97	–0.99	1.01	–1	0.96	–1.02

The identified modal mass:

$$[\Phi_{perfect}]\times[M]\times[\Phi'_{perfect}]=\begin{bmatrix} 18.16 & 0.04 & -0.15 & 0.03 & 0.12 & 0.01 \\ 0.04 & 5.71 & 0 & 0.01 & 0.05 & 0 \\ -0.14 & 0 & 3.69 & -0.01 & 0.10 & -0.03 \\ 0.03 & 0.01 & -0.01 & 3.67 & 0.04 & -0.01 \\ 0.12 & 0.05 & 0.10 & 0.04 & 5.32 & 0.02 \\ 0.01 & 0 & -0.03 & -0.01 & 0.02 & 18.73 \end{bmatrix}$$

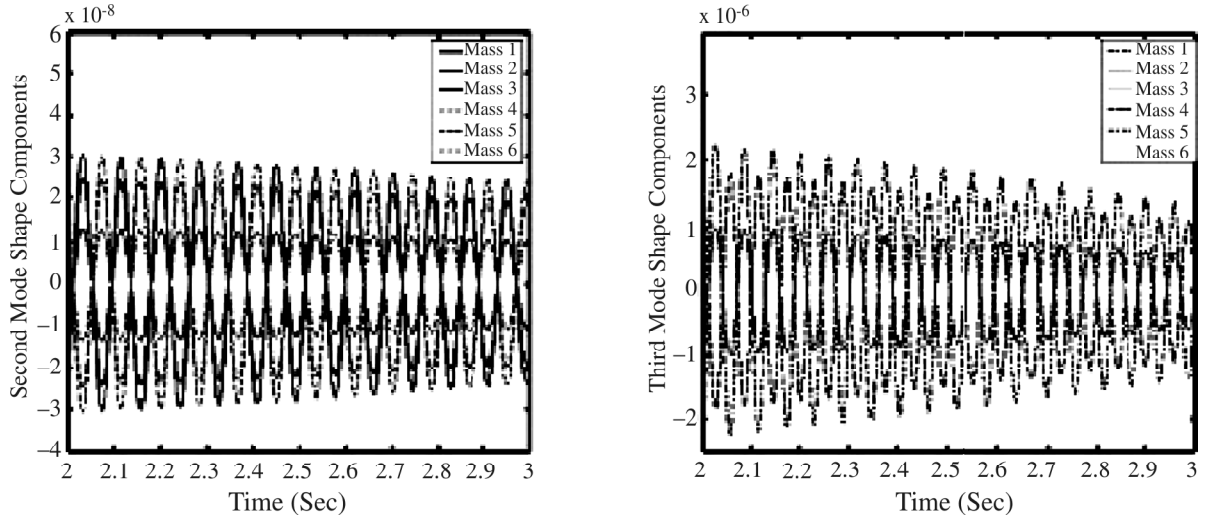

Figure (6): Plots of (a) the Second Modal Response, (b) the Third Modal Response of the Mechanical System

The identified stiffness matrix:

$$K_{perfect} = \Phi^{-1} \times diag[K_j] \times [\Phi^{-1}]' = \begin{bmatrix} 14684 & -7327 & -128 & -153 & 131 & -188 \\ -7327 & 15176 & -7381 & -56 & 418 & -3 \\ -128 & -7381 & 14743 & -7537 & -139 & 13 \\ -153 & -56 & -7537 & 14744 & -7443 & -4 \\ 131 & 418 & -139 & -7443 & 15229 & -7430 \\ -188 & -3 & 13 & -4 & -7430 & 14885 \end{bmatrix}$$

The theoretical stiffness matrix:

$$K_{theory} = \begin{bmatrix} 15000 & -7500 & 0 & 0 & 0 & 0 \\ -7500 & 15000 & -7500 & 0 & 0 & 0 \\ 0 & 0 & -7500 & 15000 & -7500 & 0 \\ 0 & 0 & 7500 & 15000 & -7500 & 0 \\ 0 & 0 & 0 & -7500 & 15000 & -7500 \\ 0 & 0 & 0 & 0 & -7500 & 15000 \end{bmatrix}$$

The identified damping matrix:

$$C = \Phi^{-1} \times diag\,[c_j] \times \Phi^{-1}]' = \begin{bmatrix} 1.4739 & -0.7331 & -0.0148 & -0.0151 & 0.0133 & -0.022 \\ -0.7331 & 1.5213 & -0.7382 & -0.0074 & 0.0389 & -0.0001 \\ -0.0148 & -0.7382 & 1.4781 & -0.7571 & -0.0158 & 0.0016 \\ -0.0151 & -0.0074 & -0.7571 & 1.4781 & -0.7445 & -0.0023 \\ 0.0133 & 0.0389 & -0.0158 & -0.7445 & 1.5266 & -0.7435 \\ -0.022 & -0.0001 & 0.0016 & -0.0023 & -0.7435 & 1.4941 \end{bmatrix}$$

The theoretical damping matrix:

$$C_{theory} = \begin{bmatrix} 1.5 & -0.75 & 0 & 0 & 0 & 0 \\ -0.75 & 1.5 & -0.75 & 0 & 0 & 0 \\ 0 & -0.75 & 1.5 & -0.75 & 0 & 0 \\ 0 & 0 & -0.75 & 1.5 & -0.75 & 0 \\ 0 & 0 & 0 & -0.75 & 1.5 & -0.75 \\ 0 & 0 & 0 & 0 & -0.75 & 1.5 \end{bmatrix}$$

As can be seen, there is good agreement between the identified and theoretically obtained results.

INTRINSIC MODE FUNCTIONS (IMFS) BASED DAMAGE DETECTION METHODS

Having demonstrated the ability of the Hilbert Transform approach in evaluating the vibration response of damage and undamaged structures, in this paper we also illustrate another application of the method, that is, damage detection in structures. For that we have introduced a novel damage index for identifying damage in a given structure. This index is based on the first IMF of the filtered signal, which is indeed very close to the modal response of the structure. The energy of the first IMF can be evaluated by:

$$E_{mn} = \int_0^{t_0} (IMF)_{mn}^2 dt \tag{16}$$

In the above equation, m is the sensor's number or the degree of freedom of the structure being considered, n is the mode shapes' number and (IMF) is the first calculated intrinsic mode function of the signal, which has been passed through the aforementioned band-pass process. The damage index is therefore defined as:

$$DI_{mn} = \left| \frac{E_{mn}^{Healthy} - E_{mn}^{Damaged}}{E_{mn}^{Healthy}} \right| \times 100 \tag{17}$$

The advantage of the proposed damage detection approach is that the approach does not require significant computational effort, since the same procedure used for establishing the stiffness and damping matrices are effectively used to establish the damage index and location. Another advantage is that only the first few modal responses of (IMFs) are required for establishing the damage location.

To illustrate the capability of the proposed approach, the same 6-DOF mechanical systems (damaged and undamaged) are again considered. The energy terms calculated based on the IMFs, and the corresponding damage indices are evaluated and tabulated in Table 3. Note that for the purpose of establishing the existence of the damage, only the first two frequencies have been used. It can be clearly seen that the energy terms

Table 3
Energy and damage indices of the first two modal responses based on the IMF energy.

Mass Number	*IMF Energy of the healthy system*		*IMF Energy of the damaged system*		*Damaged Indices*	
	First Mode	*Second Mode*	*First Mode*	*Second Mode*	*First Mode*	*Second Mode*
1	1.3562	.12167	1.3728	.23541	1.22	93.48
2	4.3844	.18827	4.4029	.5358	0.42	186.64
3	6.853	.036594	6.8652	.38273	0.18	**945.88**
4	6.9479	.038671	6.8919	.39534	0.81	**922.32**
5	4.4425	.18963	4.4302	.5416	0.28	185.60
6	1.3565	.12149	1.361	.23685	0.33	94.95

corresponding to the first mode of the system have remained stationary for the undamaged and the damaged system. However, the results of Table 3 indicate that the energy terms corresponding to the second mode shape have significantly changed. Moreover, the maximum difference in the energy terms is in the vicinity of DOF three and four.

CONCLUSIONS

A theoretical investigation was carried out to investigate the vibration characteristics of a six degree freedom mechanical system. The investigation was carried out to demonstrate the capability and integrity of Empirical Modal Decomposition (EMD) with respect to assessing performance of structures, in healthy and damage states. Some of the more significant observations from this study are summarized below:

1. The Hilbert-Huang spectral analysis method could be effectively used for the identification of the dynamic characteristics of multi-DOF structural systems.
2. The natural frequencies and damping ratios of the system could be effectively calculated based on the data collected through only one single sensor used for measuring the free vibration-time history of the system (more importantly, only at one single location).
3. Establishing the above information for a healthy system, as well as a damaged system can also effectively establish the presence of damage and its location by way of the proposed damage index. The developed damage index is based on the first intrinsic mode function.

ACKNOWLEDGEMENTS

The financial support of the Atlantic Innovation fund, as well as NSERC granted to the second author in support of this work is gratefully acknowledged. The Killam Scholarship awarded to the first author is also acknowledged and appreciated.

REFERENCES

[1] Cheraghi, N., Vibation-Based Damage Detection of Structures Using Signal Analysis Methods. Doctoral Thesis, Faculty of Engineering, Dalhousie University, Halifax, NS, Canada (2006).

[2] Deng, Y., Wang W., Qian C. and Dai, D., Boundary-Processing Technique in EMD Method and Hilbert Transform. *Chinese Science Bulletin*, **46**(3), (2001), 954–961.

[3] Doebling, S. W., Farrar, C. R., Prime, M. B. and Shevitz, D. W., (1996) Damage Identification and Health Monitoring of Structural and Mechanical Systems from Changes in their Vibration Characteristics: A Literature Review, Los Alamos National Laboratory report LA-13070-MS.

[4] Flandrin, P., Rilling, G. and Goncalves, P., Empirical Mode Decomposition as a Filter Bank. *IEEE Signal Processing Letters*, **11**(2), (2004), 112–114.

[5] Hahn, S. J. The Hilbert Transform of the Product a(t) cos(ωt + '0). *Bulletin of the Polish Academy of Science* **44**(1), (1996), 75–80.

[6] Han, C., Guo, H., Wang, C , Fan. D, and Sang,. H., Multiscale Edge Detection Based on EMD. *High Technology Letters (Chinese version)*, **6**, (2003), 13–17.

[7] Hilbert-Huang Transform to the Analysis of Molecular Dynamic Simulations. *J. Phys. Chem.*, A (107): 4869–4876.

[8] Huang *et al.*, "The Empirical Mode Decomposition Method and the Hilbert Spectrum for Non-linear and Non-stationary Time Series Analysis", Proc. R. Soc. Lond , **454**, (1998), 903-995.

[9] Huang, N. E., Shen, Z., Long, S. R., Wu, M. C., and Shih, H. H., The Empirical Mode Decomposition and Hilbert Spectrum for Nonlinear and Non-stationary Time Series Analysis. Proceedings of the Royal Society of London—Series A **454**, (1998), 903–995.

[10] Huang, N.E., Shen, Z., and Long, S.R., A New View of Nonlinear Water Waves: the Hilbert Spectrum. *Ann Rev Fluid Mech*, **31**, (1999), 417–457.

[11] Huang, N. E., Applications of Hilbert-Huang Transformation for Speech and Vibration Signal Analysis. Proceedings of the Tenth International Congress on Sound and Vibration, the Tenth International Congress on Sound and Vibration: (2003), 4223-4230

[12] Huang, W., Shen, Z., Huang, N. E., and Fung, Y. C., Engineering Analysis of Biological Variables: An Example of Blood Pressure Over 1 day. *Proc. Natl. Acad. Sci. USA*, **95**, (1998), 4816–4821.

[13] Loh, C. H., Wu, T. C., and Huang, N. E. (2001), Application of EMD+HHT Method to Identify Near-fault Ground Motion Characteristics and Structural Responses. *BSSA*, Special.

[14] Nunes, J. C., Bouaoune, Y., Delechelle, E., Niang, O., and Bunel, P. H., Image Analysis by Bidimensional Empirical Mode Decomposition. *Image and Vision Computing*, **21**, (2003), 1019–1026.

[15] Phillips, S. C., Gledhill, R. G., Essex, J. W., and Edge, C. M. (2003) Application of theTitchmarsh. EC (1948) *Introduction to the Theory of Fourier Integrals*. Oxford University Press.

[16] Titchmarsh, E. C. 1948 *Introduction to the theory of Fourier integrals*. Oxford University Press.

[17] Xu, Y. L., Asce, M., and Chen, J., Structural Damage Detection Using Empirical Mode Decomposition: Experimental Investigation, *Journal of Engineering Mechanics*, November, **130**, (2004), 1279-1288.

[18] Yang, J. N. and Lei, Y. (2000), Identification of Civil Structures with Non-proportional Damping In Smart Structures and Materials 2000: Smart Systems for Bridges, Structures and Highways. Proceedings of SPIE, 3988, Newport Beach, CA, 284–294.

N. Cheraghi
Colt Engineering Corporation
Calgary, AL, Canada

F. Taheri
Department of Civil and Resource Engineering
Dalhousie University, 1360 Barrington Street
Halifax, Nova Scotia B3J 1Z1, Canada
E-mail: farid.Taheri@dal.ca